



Article

The ϵ -Isozyme of Protein Kinase C (PKC ϵ) Is Impaired in ALS Motor Cortex and Its Pulse Activation by Bryostatin-1 Produces Long Term Survival in Degenerating SOD1-G93A Motor Neuron-like Cells

Valentina La Cognata ^{1,†}, Agata Grazia D'Amico ^{2,†}, Grazia Maugeri ² , Giovanna Morello ¹, Maria Guarnaccia ¹, Benedetta Magri ², Eleonora Aronica ³ , Daniel L. Alkon ⁴, Velia D'Agata ² and Sebastiano Cavallaro ^{1,*}

¹ Institute for Biomedical Research and Innovation, National Research Council, 95126 Catania, Italy

² Section of Human Anatomy and Histology, Department of Biomedical and Biotechnological Sciences, University of Catania, 95123 Catania, Italy

³ Department of (Neuro) Pathology, Amsterdam UMC, University of Amsterdam, Amsterdam Neuroscience, Meibergdreef 9, 1105 Amsterdam, The Netherlands

⁴ Synaptogenix, Inc., New York, NY 10036, USA

* Correspondence: sebastiano.cavallaro@cnr.it

† These authors contributed equally to this work.



Citation: La Cognata, V.; D'Amico, A.G.; Maugeri, G.; Morello, G.; Guarnaccia, M.; Magri, B.; Aronica, E.; Alkon, D.L.; D'Agata, V.; Cavallaro, S. The ϵ -Isozyme of Protein Kinase C (PKC ϵ) Is Impaired in ALS Motor Cortex and Its Pulse Activation by Bryostatin-1 Produces Long Term Survival in Degenerating SOD1-G93A Motor Neuron-like Cells. *Int. J. Mol. Sci.* **2023**, *24*, 12825. <https://doi.org/10.3390/ijms241612825>

Academic Editor: Claudia Ricci

Received: 11 July 2023

Revised: 12 August 2023

Accepted: 14 August 2023

Published: 15 August 2023



Copyright: © 2023 by the authors. Licensee MDPI, Basel, Switzerland. This article is an open access article distributed under the terms and conditions of the Creative Commons Attribution (CC BY) license (<https://creativecommons.org/licenses/by/4.0/>).

Abstract: Amyotrophic lateral sclerosis (ALS) is a rapidly progressive and ultimately fatal neurodegenerative disease, characterized by a progressive depletion of upper and lower motor neurons (MNs) in the brain and spinal cord. The aberrant regulation of several PKC-mediated signal transduction pathways in ALS has been characterized so far, describing either impaired expression or altered activity of single PKC isozymes (α , β , ζ and δ). Here, we detailed the distribution and cellular localization of the ϵ -isozyme of protein kinase C (PKC ϵ) in human postmortem motor cortex specimens and reported a significant decrease in both PKC ϵ mRNA (*PRKCE*) and protein immunoreactivity in a subset of sporadic ALS patients. We furthermore investigated the steady-state levels of both pan and phosphorylated PKC ϵ in doxycycline-activated NSC-34 cell lines carrying the human wild-type (WT) or mutant G93A SOD1 and the biological long-term effect of its transient agonism by Bryostatin-1. The G93A-SOD1 cells showed a significant reduction of the phosphoPKC ϵ /panPKC ϵ ratio compared to the WT. Moreover, a brief pulse activation of PKC ϵ by Bryostatin-1 produced long-term survival in activated G93A-SOD1 degenerating cells in two different cell death paradigms (serum starvation and chemokines-induced toxicity). Altogether, the data support the implication of PKC ϵ in ALS pathophysiology and suggests its pharmacological modulation as a potential neuroprotective strategy, at least in a subgroup of sporadic ALS patients.

Keywords: PKC ϵ ; *PRKCE*; amyotrophic lateral sclerosis; neurodegeneration; Bryostatin-1

1. Introduction

Amyotrophic lateral sclerosis (ALS) is a fatal adult-onset neurodegenerative disorder characterized by the progressive degeneration of upper and lower motor neurons (MNs) in the cortex, brainstem and spinal cord. Motor neuron deterioration results in muscle weakness and, ultimately, in death due to respiratory failure, typically within 3–5 years after diagnosis [1,2].

The majority of cases (90%) are sporadic (SALS) without a family history, while the remaining 10% of ALS patients are inherited (familial ALS or FALS) [1,3,4]. Approximately 12% of familial cases and 2% of sporadic ALS cases are caused by mutations in the Cu/Zn superoxide dismutase 1 (*SOD1*) gene, one of the first discovered ALS genes [5–8]. The clinical presentation of SALS and FALS are similar, and treatment options remain

primarily supportive so far. Indeed, the two current FDA-approved drugs, i.e., the anti-excitotoxic Riluzole (Rilutek) and the antioxidant Edaravone, are able to extend the lifespan of patients by a few months and counteract disease progression without a real resolute outcome [9,10].

The pathogenic process underlying ALS neurodegeneration is multifactorial and still not fully determined, although dysfunctions in several cellular and molecular processes have been reported so far, including impaired protein homeostasis, mitochondrial alterations, aberrant RNA metabolism, neuroinflammation, excitotoxicity and oxidative stress [11]. In the last few years, our research group and others have demonstrated that sporadic ALS is a phenotypically and genetically heterogeneous disease, and SALS patients may be taxonomized into distinct molecular subtypes based on postmortem motor cortex transcriptomic signatures [11–16]. This evidence emphasized the idea that molecular-based studies aimed at uncovering the disease etiopathogenesis, as well as at characterizing biomarkers or effective treatments, require updating and necessitate accurate stratified case monitoring [11].

Multiple studies have implicated deregulation in ALS of the protein kinase C (PKC)-mediated signal transduction mechanisms, through changes in either the expression or activity state of several members of the PKC superfamily [17–22]. This latter consists of 10 related serine/threonine protein kinases (isozymes) that can be grouped into three subclasses, according to structural motifs and activation requirements: (i) classical (also termed conventional) cPKCs (α , β and γ) require both diacyl glycerol (DAG) and a calcium ion for activation, (ii) novel nPKCs (δ , ϵ , η and θ) require DAG but not by calcium [23], and (iii) atypical aPKCs (ζ and τ/γ) are insensitive to calcium and DAG but are activated by other lipids or by phosphorylation [23,24].

The novel ϵ isoform (PKC ϵ) is a finely regulated enzyme known for its important roles in the nervous [25,26], cardiac [27] and immune systems [28]. Currently, it represents an attractive target for the treatment of several conditions, such as inflammation, ischemia, addiction, pain, anxiety and cancer [24], and has recently gained attention in Alzheimer's disease (AD) for its role in both memory formation and regulation of β -amyloid misfolded proteins [29,30]. The PKC ϵ enzyme shares many structural features with the other members of the PKC family, including the DAG (C1) and the C2-like phospholipid-binding domains, the pseudo-substrate (PS) site, the catalytic terminal C3 and C4 domains containing the ATP binding site, the substrate recognition site and the kinase domain [24]. Like the other PKC isozymes, PKC ϵ must be primed through phosphorylation to display full enzymatic activity and respond to allosteric regulators. Phosphorylation can occur at three conserved sites in the catalytic domain: the activation loop (Thr-566), the Thr-Pro turn motif (Thr-710) and the hydrophobic Phe-Ser-Tyr motif (Ser-729) [24]. Following activation, PKC ϵ translocates into specific subcellular compartments (e.g., perinuclear/Golgi site) and changes the substrate kinetics [31].

One of the most potent PKC ϵ activators is the marine natural product Bryostatin-1, a macrocyclic lactone originally isolated from *Bugula neritina*. This molecule has long been investigated in neuroscience for its interesting ameliorative effects on neuronal structure and function in *in vitro* studies, as well as for the pro-cognitive and antidepressant outcomes *in vivo* in animal models, thus entering into human clinical trials for treating AD [32,33]. Bryostatin-1 produces a time-dependent biphasic effect on PKC ϵ levels: firstly, it binds and activates PKC ϵ , promoting its translocation from cytosol to membrane fractions [34]; then, PKC ϵ is proteolytically degraded during the so-called downregulation step and, lastly, undergoes a phase of *de novo* protein synthesis which restores PKC ϵ normal levels and induces the production of additional trophic factors (e.g., BDNF) [32,34].

The aberrant regulation of α , β , ζ and δ PKC isozymes in ALS has been previously described [17–22,35,36], but nothing is known about the contribution of the ϵ isoform in the ALS pathophysiology. In the present work, we investigated the PKC ϵ mRNA (*PRKCE*) expression level and the PKC ϵ protein cellular expression and localization in human postmortem motor cortex specimens from control and ALS patients' subtypes.

Furthermore, we evaluated the steady-state levels of pan and phosphorylated PKC ϵ in murine NSC-34 motor neuron-like cells expressing human wild-type (WT) or mutant G93A-SOD1 [37] and inspected the biological long-term effect of PKC ϵ activation by Bryostatin-1.

2. Results

2.1. PKC ϵ Is Expressed by Different Cell Types in Human Primary Motor Cortex

In order to understand the biological role of PKC ϵ in the pathophysiology of the human motor cortex, we first investigated its cellular distribution in postmortem cortical specimens from control patients by fluorescence immunohistochemistry. Double labeling with fluorescent antibodies revealed a widely panPKC ϵ immunoreactivity in the cortical neurons (MAP2⁺ or NF-H⁺), microglial cells (CD11b⁺) and oligodendrocytes (OLIG2⁺), but barely in the astrocytes (GFAP⁺) (Figures 1 and 2).

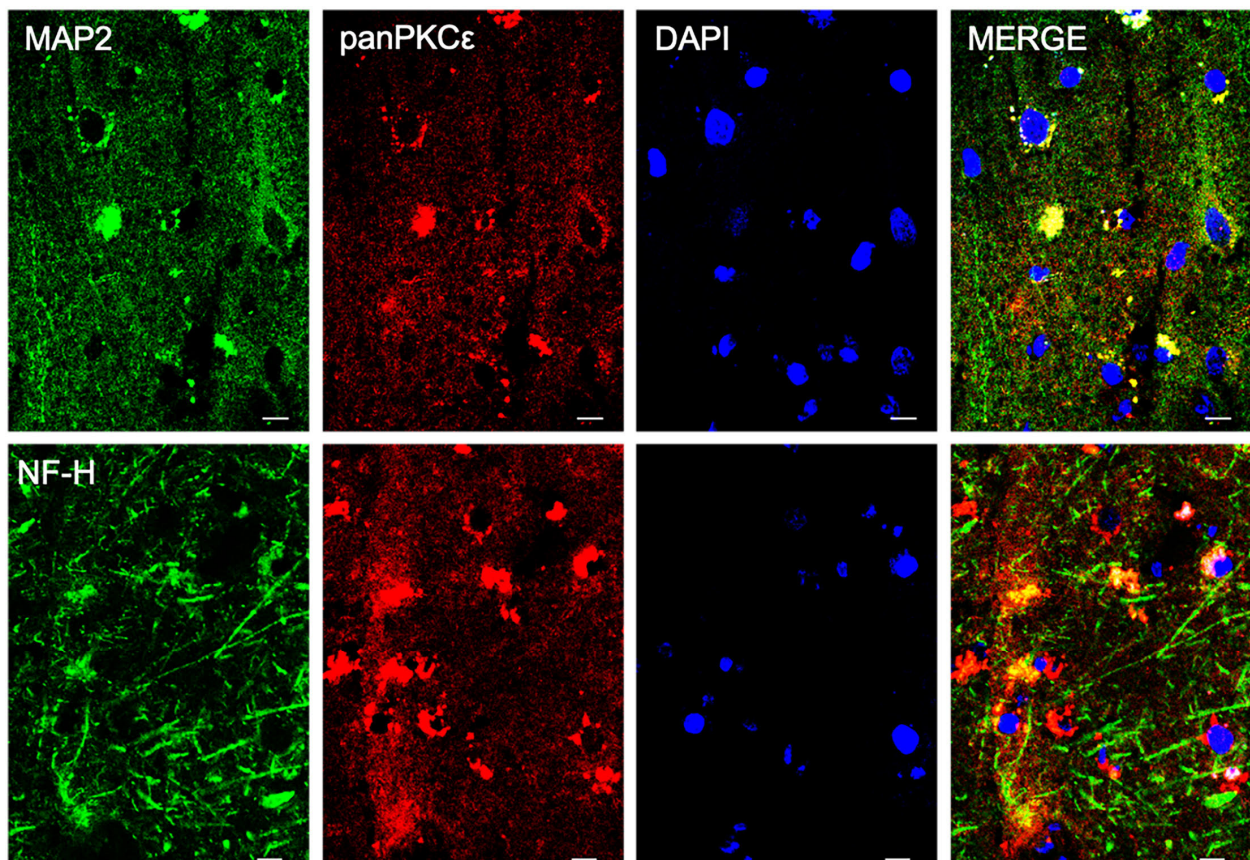


Figure 1. PKC ϵ is expressed by cortical neurons in human primary motor cortex. Representative photomicrographs show panPKC ϵ expressed in cortical neuronal cells (MAP2⁺ or NF-H⁺) examined under a Nikon A1 confocal inverted microscope equipped with a Plan Apochromat lambda 60 \times /1.4 oil immersion lens (Nikon, Tokyo, Japan). Scale bar 10 μ m.

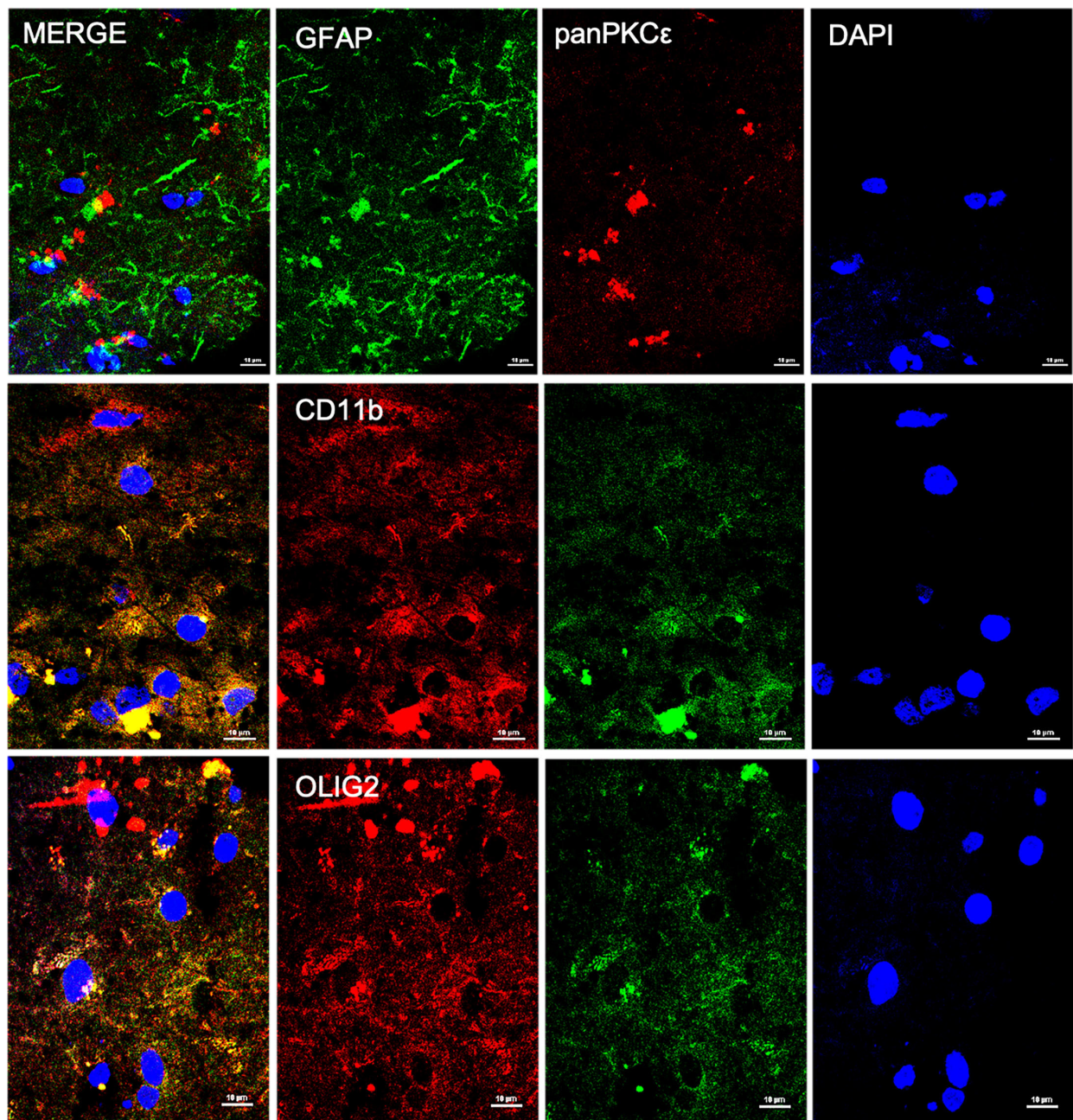


Figure 2. PKC ϵ is expressed by non-neuronal cells in human primary motor cortex. Representative photomicrographs show panPKC ϵ expressed in microglial cells (CD11b⁺) and oligodendrocytes (OLIG2⁺) but barely in astrocytes (GFAP⁺). Slides were examined under a Nikon A1 confocal inverted microscope equipped with a Plan Apochromat lambda 60 \times /1.4 oil immersion lens (Nikon, Tokyo, Japan). Scale bar 10 μ m.

2.2. PRKCE mRNA Expression Level Is Reduced in Motor Cortex in a Subset of ALS Patients

To characterize the biological significance of PKC ϵ in ALS, we first compared the expression level of PKC ϵ encoding-gene (*PRKCE*) in control and ALS motor cortex subgroups from two independent RNA gene-expression studies.

The first analysis relied on the E-MTAB-2325 transcriptomic dataset, which collected the whole-genome microarray RNA profiles of the motor cortex from 31 sporadic ALS samples and 10 controls. The previous examination of these RNA profiles had revealed a clear transcriptional-based clustering of subjects into three distinct groups: control ($n = 10$), SALS1 ($n = 18$) and SALS2 ($n = 13$) subtypes, each associated with different molecular

features and potential drug targets [14,16,38]. Among the multiple differentially expressed genes, *PRKCE* emerged as significantly decreased in SALS2 (not in SALS1) patients compared to the controls (Figure 3a).

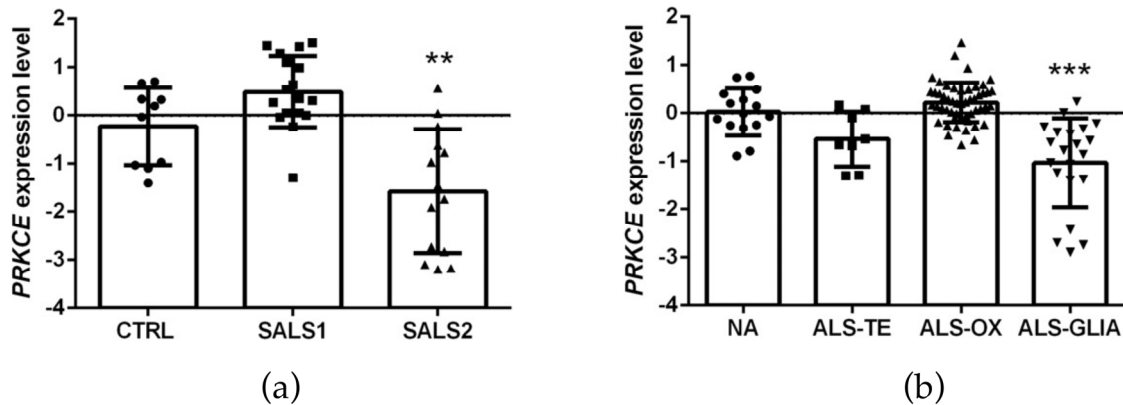


Figure 3. PKC ϵ mRNA (*PRKCE*) is downregulated in motor cortex in a subset of sporadic ALS patients. (a). Transcriptomic data extrapolated from E-MTAB-2325 dataset showing a statistically significant downregulation of *PRKCE* mRNA expression level in motor cortex in a subset of sporadic ALS patients (SALS2) compared to CTRL (control = 10, SALS1 = 18, SALS2 = 13 patients, respectively). (b). Transcriptomic data derived from GSE124439 dataset showing a statistically significant downregulation of *PRKCE* mRNA expression level in motor cortex in a subset of ALS patients (ALS-Glia) compared to non-neurological controls (NA) (NA = 15, ALS-TE = 8, ALS-OX = 51, ALS-Glia = 21 patients, respectively). Data were extrapolated from ArrayExpress (<http://www.ebi.ac.uk/arrayexpress/> accessed on 1 June 2021) and Gene Expression Omnibus (<https://www.ncbi.nlm.nih.gov/geo/> accessed on 1 January 2023), respectively, and analyzed as described in the Materials and Methods section. Tukey–Kramer post hoc test: ** $p < 0.01$ vs. CTRL, *** $p < 0.001$ vs. NA. Circles, squares or triangles indicate the *PRKCE* expression level of single patients for each experimental group from the two datasets.

To corroborate this observation, we further explored the cortical *PRKCE* mRNA level in a second bulk transcriptome study (i.e., the GSE124439 dataset), which profiled by RNA-sequencing 80 ALS and 15 non-neurological control (NA) motor cortex areas (both medial and lateral) [15], and stratified the ALS patients into three distinct molecular subtypes: (i) ALS-TE, marked by retrotransposon re-activation as a dominant feature ($n = 8$); (ii) ALS-OX, showing evidence of oxidative and proteotoxic stress ($n = 51$); (iii) ALS-Glia, with strong signatures of glial activation and inflammation ($n = 21$) [15]. Interestingly, a significant downregulation of *PRKCE* mRNA was observed only in the ALS-Glia patients (Figure 3b).

2.3. PKC ϵ Immunoreactivity Is Decreased in Both ALS Postmortem Primary Motor Cortex and SOD1-G93A NSC-34 Cells

To characterize the global protein expression and phosphorylation state of PKC ϵ in the human control and SALS2 motor cortex samples, we performed fluorescent immunohistochemistry studies. Staining with both anti-panPKC ϵ and anti-phospho-S729-PKC ϵ antibodies revealed an overall decreased immunoreactivity for both antibodies in the motor cortex (NF-H⁺ area) of SALS2 patients compared to controls (Figure 4).

Considering that the SALS2 subcluster was the only one showing significant deregulation in SOD1 expression level [16,38], we decided to inspect PKC ϵ expression in vitro in the widely used murine cellular humanized ALS model, i.e., NSC-34 over-expressing WT or mutated human SOD1-G93A under doxycycline activation, as previously reported [39]. Consistent with the human-derived motor cortex data, we detected a downregulation of the panPKC ϵ and phosphoPKC ϵ immunoreactivity in G93A NSC-34 cells compared to WT (Figure 5) and used this model for the following studies.

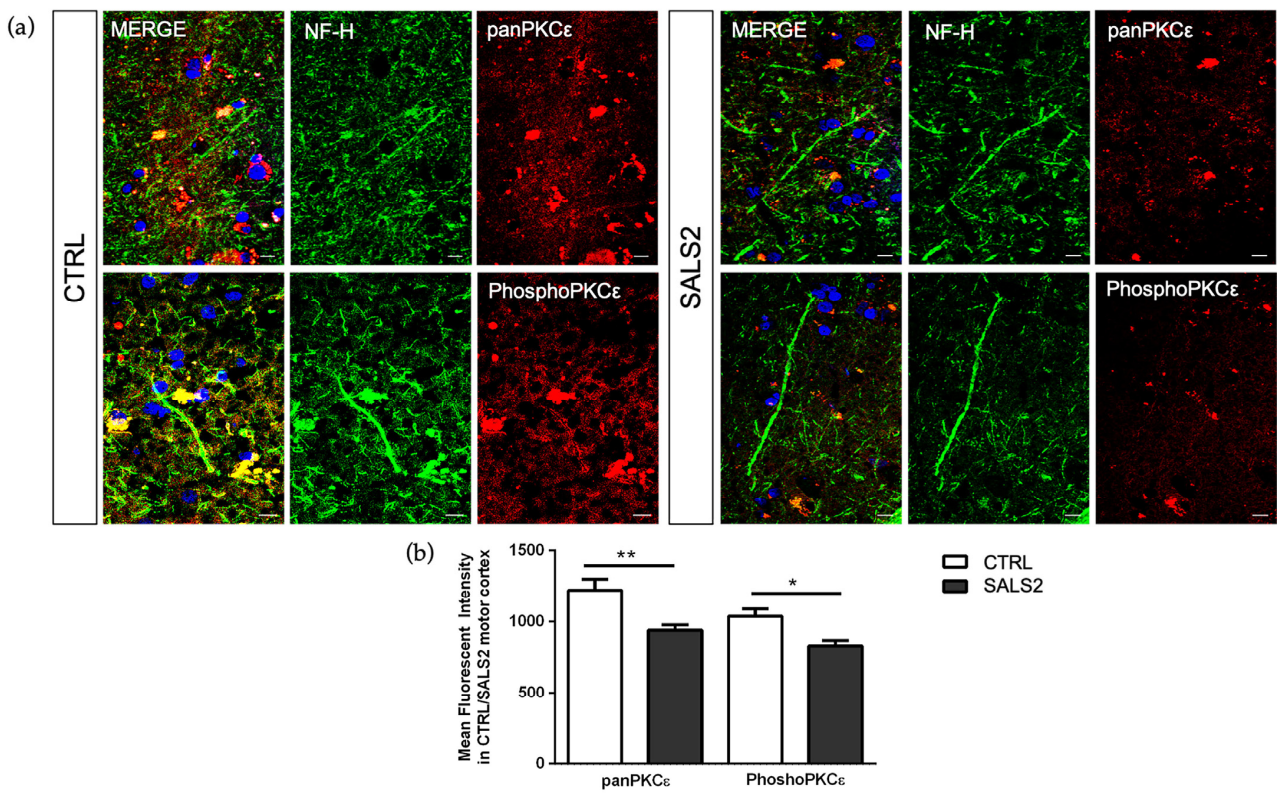


Figure 4. The panPKCε and phosphoPKCε levels are reduced in motor cortex area of SALS2 patients. (a). Representative images showing panPKCε and phosphoPKCε immunoreactivity in motor cortex area (characterized by NF-H positive staining) of control and SALS2 patients. (b). Fluorescence mean intensity, quantified by examining samples under a Nikon A1 confocal inverted microscope equipped with a Plan Apochromat lambda 60×/1.4 oil immersion lens (Nikon, Tokyo, Japan). The mean intensity of TRITC channel was extrapolated from multiple regions of interest (ROI) and normalized to the background by using the NIS-Elements AR (Advanced Research) software (version 4.60). Scale bar 10 μm. Tukey–Kramer post hoc test: ** $p < 0.01$ SALS2 vs CTRL for panPKCε, * $p < 0.05$ SALS2 vs. CTRL for phosphoPKCε.

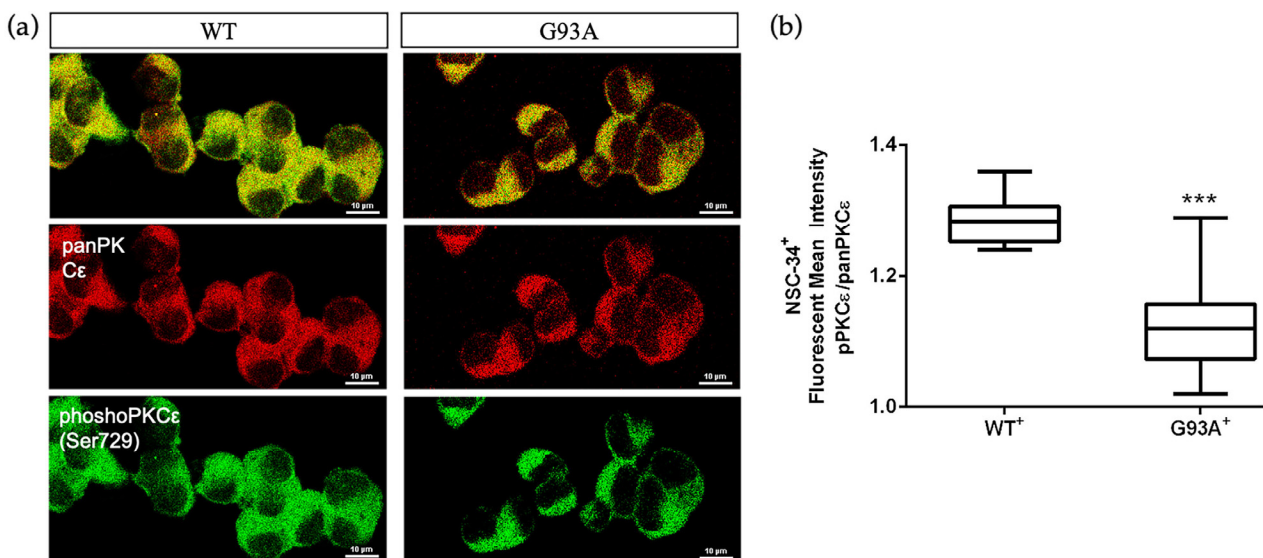


Figure 5. Immunoreactivity ratio of phosphoPKCε/panPKCε is reduced in SOD1-G93A NSC-34 cells. (a). Representative images showing panPKCε and phosphoPKCε immunoreactivity in WT and

SOD1-G93A NSC-34 cells. (b). Fluorescence mean intensity, quantified by examining samples under a Nikon A1 confocal inverted microscope equipped with a Plan Apochromat lambda 60×/1.4 oil immersion lens (Nikon, Tokyo, Japan). The mean intensity of each channel was extrapolated from multiple regions of interest (ROI) and normalized to the background by using the NIS-Elements AR (Advanced Research) software (version 4.60). Scale bar 10 μm. Tukey–Kramer post hoc test: *** $p < 0.001$ vs. WT.

2.4. A Pulse Activation by Bryostatin-1 Promotes Long-Term Cell Survival in Degenerating SOD1-G93A NSC-34 Cells and Changes the phosphoPKC ϵ /panPKC ϵ Ratio

Based on the observed PKC ϵ downregulation in the ALS condition, we wondered about the downstream pharmacological effects of PKC ϵ agonism in vitro and examined the biological outcomes of PKC ϵ pulse activation by Bryostatin-1 in WT and G93A NSC-34 cells in two different paradigms of cell death models. Induction to apoptosis in both WT and G93A doxy-activated cells was prompted by: (i) serum starvation at either 24 or 48 h, or (ii) co-incubation with toxic chemokines (i.e., MIP2 α and GRO α) for 48 h. This second apoptosis model derives from previous observations conducted in our laboratories [40], which highlighted the vulnerability of G93A cells to MIP2 α and GRO α ligand treatment. Indeed, in the chemokines-induced cell death paradigm, the G93A NSC-34 cells displayed more sensitivity to apoptosis compared to the WT NSC-34, showing a peculiar significant reduction of cell viability in the presence of GRO α and MIP2 α (Figure 6b).

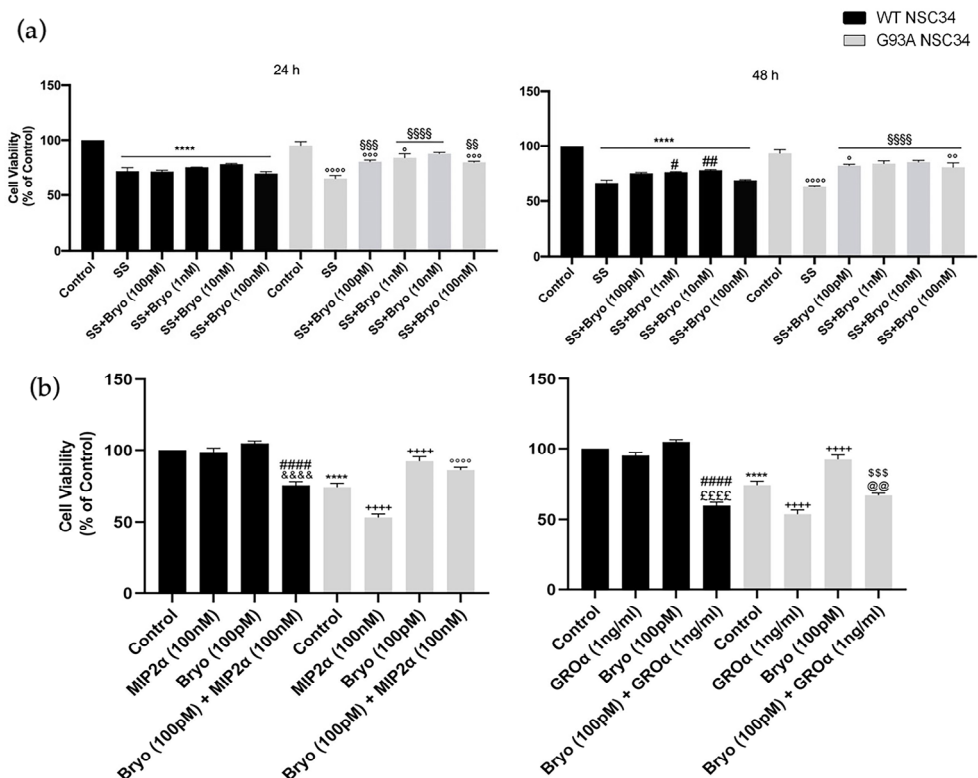


Figure 6. A pulse activation of PKC ϵ by Bryostatin-1 produces long-term survival in degenerating mutant SOD1-G93A cells. (a). Cell viability of WT and SOD1-G93A NSC-34 cultured in normal growth medium (Control), serum starvation (ss) and exposed at different concentrations of Bryostatin-1 for 10 min after 24 and 48 h. Normal growth medium-cultured cells were used as controls. Results are representative of at least three independent experiments and values are expressed as a percentage of control (**** vs. Control WT, ° or °° or °°° or °°°° vs. Control G93A, # or ## vs. SS WT, SS or SS° or SS°° vs. SS G93A as determined by one-way ANOVA followed by Tukey–Kramer post hoc test). (b). Cell viability of WT and SOD1-G93A NSC-34 cultured for 48 h in normal growth medium (Control), in combination with toxic chemokines (GRO α and MIP2 α) and exposed to Bryostatin-1 (100 pMol) for

10 min. Normal growth medium-cultured cells were used as controls. Results are representative of at least three independent experiments and values are expressed as a percentage of control (*** $p < 0.0001$ vs. control WT, ++++ $p < 0.0001$ vs. control G93A, #### $p < 0.0001$ vs. Bryo WT, \$\$\$ $p < 0.001$ vs. Bryo G93A, °°°° $p < 0.0001$ vs. MIP2 α G93A, &&&& $p < 0.0001$ vs. MIP2 α WT, ££££ $p < 0.0001$ vs. GRO α WT, @@ $p < 0.0001$ vs. GRO α G93A as determined by one-way ANOVA followed by Tukey–Kramer post hoc test).

The cells were then exposed to a pulse treatment (10 min) with Bryostatin-1. We used increasing concentrations of Bryostatin-1 (100 pM, 1 nM, 10 nM and 100 nM) in the serum deprivation condition (Figure 6a) and a single dose (100 pM) in the chemokines-induced toxicity paradigm (Figure 6b). In both apoptotic paradigms, the PKC ϵ pulse activation by Bryostatin-1 determined a significant increase in cellular viability in degenerating G93A NSC-34 cells compared to the untreated controls (Figure 6a).

Previous data on Bryostatin-1 showed it produces a time-dependent biphasic effect on PKC ϵ levels since it immediately binds PKC ϵ promoting its self-phosphorylation and translocation from cytosol to membrane fractions [34,41], and then the enzyme undergoes a downregulation phase for several hours, followed by de novo synthesis. We therefore measured PKC ϵ immunoreactivity after 48 h from Bryostatin-1 pulse activation and, concordantly with previous observations, detected late decreased levels of the phosphoPKC ϵ /panPKC ϵ ratio in both the WT and G93A NSC-34 cells (Figure 7).

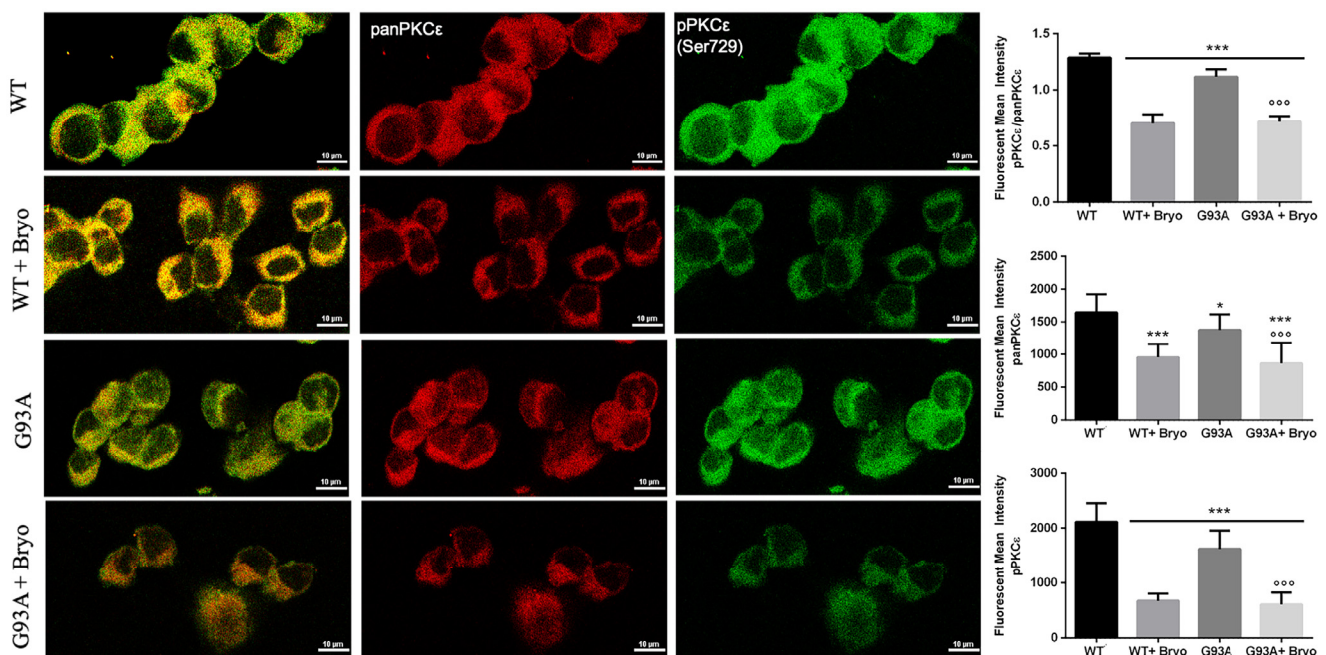


Figure 7. A transient treatment with Bryostatin-1 induces reduction of PKC ϵ expression level in both WT and SOD1-G93A cells. Representative images showing panPKC ϵ and phosphoPKC ϵ immunoreactivity in WT and SOD1-G93A NSC-34 cells after 48 h from the 10 min pulse activation by Bryostatin-1. Fluorescence was quantified by examining samples under a Nikon A1 confocal inverted microscope equipped with a Plan Apochromat lambda 60 \times /1.4 oil immersion lens (Nikon, Tokyo, Japan). The mean intensity of each channel was extrapolated from multiple regions of interest (ROI) and normalized to the background by using the NIS-Elements AR (Advanced Research) software (version 4.60). Scale bar 10 μ m. Tukey–Kramer post hoc test: *** $p < 0.001$ or * $p < 0.05$ vs. WT, °°° $p < 0.001$ vs. G93A.

3. Discussion

The mechanisms underlying motor neuron cell death and axonal degeneration in ALS still remain elusive, partly due to our incomplete knowledge of the biological mechanisms

controlling neuronal degeneration. In this study, we focused our attention on the ϵ -isozyme of PKC (PKC ϵ), a versatile enzyme regulating a number of cellular processes including proliferation, differentiation, chemotaxis, neurogenesis of cortical area, outgrowth of neurites, memory, synaptic growth and synaptogenesis, and mitochondria-mediated regulation of free radical production and apoptosis [17,42–46].

PKC ϵ is widely expressed throughout the body, predominantly in brain regions [25,36,47] such as the hippocampus, Calleja's islands, olfactory tubercle, cerebral cortex, septal nuclei, nucleus accumbens, frontal cortex, striatum and caudate putamen [45]. In the present study, we detailed PKC ϵ distribution in the postmortem human primary motor cortex, describing its expression in cortical neurons (MAP2⁺ or NF-H⁺), microglial cells (CD11b⁺) and oligodendrocytes (OLIG2⁺), but barely in astrocytes (GFAP⁺).

Despite a number of former studies highlighted a significant deregulation of other PKC-isozymes (α , β , ζ and δ) in the motor neurons of ALS patients and in SOD1-G93A murine models [17–19,35,36], no previous studies have investigated the role of the ϵ -isozyme in ALS pathophysiology. Here, we observed that PKC ϵ mRNA expression level does not show differences when ALS is considered as a single entity, while it displays a significant downregulation in particular molecular subtypes of sporadic ALS patients obtained by bulk transcriptomic-based profiling (SALS2 from Aronica et al. [16] and ALS-Glia subset from Tam et al. [15]). Then, focusing the immunofluorescence analysis on postmortem SALS2 primary motor cortex areas, we disclosed a concordant significant downregulation of both panPKC ϵ and phospho-Ser729-PKC ϵ expression compared to the controls. Such PKC ϵ downregulation may be the result of the selective motor neuronal depletion in terminal ALS patients, which are usually characterized by extensive astrocytosis.

As previously described, the SALS2 subcluster was the only one showing significant deregulation of the *SOD1* expression level [16,38]. Therefore, we decided to inspect PKC ϵ -mediated biological effects in an ALS in vitro model characterized by overexpression of WT and mutant SOD1, i.e., NSC-34 carrying WT or mutated human SOD1 (G93A). Consistent with the human-derived motor cortex data, we detected a downregulation of phosphoPKC ϵ /panPKC ϵ ratio immunoreactivity in G93A NSC-34 cells compared to WT.

Given the decreased PKC ϵ expression and its impaired phosphorylation state in ALS, we investigated the long-term biological effect of Bryostatin-1, a macrolide lactone and potent agonist of PKC ϵ [32] in both WT and G93A NSC-34 motor neuron-like cells [37], triggered to death by two different apoptotic ways (growth factor starvation and chemokines-induced toxicity). The in vitro assays revealed that a PKC ϵ pulse activation treatment (10 min) by Bryostatin-1 plays a long-term neuroprotective action in degenerating cells, especially in the G93A background. This finding is in agreement with previous studies showing that Bryostatin-1 increases cortical synaptogenesis and is useful in enhancing learning and memory in preclinical models of AD [32,33,48]. Moreover, the transient brief activation was sufficient to prompt a shift down of the phosphoPKC ϵ /panPKC ϵ ratio level in both WT and mutant G93A NSC-34 cells, a finding that could represent the well-documented downregulation phenomenon resulting from PKC ϵ C1 domain activation in neurons [32,49–51].

Of course, the study has several limitations, such as the unknown precise time course of PKC ϵ turnover, and the used murine cell-based model, which does not exhaustively recapitulate the complex ALS portrait. Nonetheless, these findings, along with the well-characterized multiplicity of PKC ϵ functions and variation in cellular and tissue distribution, could raise some interesting considerations about the contribution of the ϵ isozyme kinase in the pathogenesis of ALS [21]. Indeed, a kinase alteration could impact the production of trophic factors (e.g., BDNF) for neuronal survival, cell cycle checkpoints regulating neuronal death and survival, axonal transport and the stimulation of excitatory amino acid receptors and Ca²⁺ channels [22]. Moreover, in other neurodegenerative diseases, Bryostatin-1 proved to revert synaptic loss and restore cognitive functions [41,52]. In Alzheimer's models and patients, for example, it is able to increase synaptogenesis

through the increase in BDNF, and, therefore, it is emerging as a potential neuroprotective treatment [41,52].

Although the mechanisms described in this work are still preliminary, and the number of analyzed patients is few, the results encourage additional preclinical and clinical investigations to guide new directions in the knowledge of ALS pathophysiology. Moreover, since deregulated expression of *SOD1* was exclusively found in SALS2 but not in SALS1 patients [16,38], and the sporadic ALS-Glia human subset shares some transcriptional signatures with murine SOD1-G93A spinal microglia [15,53], SOD1-G93A NSC-34 may represent a suitable preclinical model to investigate a distinct subset of ALS human pathology.

4. Materials and Methods

4.1. Transcriptomic Profiling

For this study, we referred to a previously described bulk transcriptome dataset [16,54] available at ArrayExpress (<http://www.ebi.ac.uk/arrayexpress/> accessed on 1 June 2021) with the accession number E-MTAB-2325 (<https://www.ebi.ac.uk/biostudies/arrayexpress/studies/E-MTAB-2325/> accessed on 1 June 2021) The dataset consists of the expression profiles of motor cortexes from SALS ($n = 31$) and control ($n = 10$) subjects produced with 4×44 K Whole Human Genome Oligo expression microarrays (Agilent Technologies, Santa Clara, CA, USA). A detailed description of the subject characteristics (origin, source code, age, gender, race, disease state, survival time from diagnosis date and postmortem interval) and experimental procedures have been previously reported [16,54,55]. Raw intensity signals from motor cortex sample hybridization were thresholded to 1, log₂-transformed, normalized and baselined to the median of all the samples by using GeneSpring GX (Agilent Technologies, Santa Clara, CA, USA). Values from probes targeting *PRKCE* were extrapolated for the following analysis.

To further investigate the *PRKCE* mRNA levels in the ALS motor cortex, we used a second independent transcriptome study (GSE124439 dataset), which profiled, by RNA sequencing, a number of frontal and motor cortex specimens from a large cohort of ALS ($n = 148$) and non-neurological (NA) subjects ($n = 28$) [15]. The data from this dataset were downloaded from the Gene Expression Omnibus (<https://www.ncbi.nlm.nih.gov/geo/> accessed on 1 January 2023), imported on GeneSpring GX (Agilent Technologies), thresholded to 1 and baselined to the median of all the samples. Signals from ALS ($n = 80$) and control ($n = 15$) primary motor cortex (both medial and lateral) samples were used for further analysis.

4.2. Fluorescent Immunohistochemistry

Postmortem frozen sections (10 μ m) of motor cortex samples from control and ALS patients were collected and processed in order to perform immunofluorescence analyses, as described elsewhere [12,16,56]. We used the following primary antibodies: anti-PKC ϵ (PA5-102580, Thermo Fisher Scientific, Waltham, MA, USA, 1:200 and sc-1681, Santa Cruz Biotechnology, Inc. Dallas, TX, USA, 1:250), anti-phospho-S729-PKC ϵ (#44-977G, Thermo Fisher Scientific, Waltham, MA, USA, 1:250), anti-MAP2 (M13-13-1500, Thermo Fisher Scientific, Waltham, MA, USA, 1:300), anti-NF-H (ab187374, Abcam, Cambridge, UK, 1:200), anti-CD11b (ab133357, Abcam, Cambridge, UK, 1:500) and anti-GFAP (MAB360, Merck Millipore, Burlington, MA, USA, 1:500). TRITC- and FITC-conjugated secondary antibodies (Goat anti-rabbit 111-025-003 and Goat anti-mouse 115-095-003, Jackson Laboratories Inc., Baltimore, PA, USA) were used for 1 h at room temperature in the dark. The slides were washed 3 times in PBS after every step, mounted with glycerol mounting medium containing DAPI and analyzed with a Nikon A1 confocal inverted microscope equipped with a Plan ApoChromat lambda 60 \times /1.4 oil immersion lens (Nikon, Tokyo, Japan). Fluorescence was quantified by analyzing the mean intensity of each channel from multiple regions of interest (ROI), normalized to the background by using the NIS-Elements AR (Advanced Research, Nikon, Tokyo, Japan) software (version 4.60).

4.3. Cell Culture

A mouse motor neuron-like hybrid NSC-34 cell line (kindly provided by Dr. Cinzia Volontè from the National Research Council, Institute for Systems Analysis and Computer Science “Antonio Ruberti”) [57] was stably transfected with the pTet-ON plasmid (Clontech, Palo Alto, CA, USA) coding for the reverse tetracycline-controlled transactivator, used to construct inducible cell lines expressing the cDNAs encoding human wild-type-SOD1 (WT) or human SOD1 mutant G93A (SOD1-G93A), as previously described [39,58], and listed hereafter as WT and G93A NSC-34 cells. The treatment with doxycycline (2 µg/mL) for 24 h was used to induce WT and mutant G93A SOD1 expression.

4.4. Immuno-Cytofluorescence

NSC-34 cells expressing human WT or SOD1-G93A were cultured on glass cover slips, fixed in 4% paraformaldehyde and processed in order to perform an immunofluorescence assay [12,59]. The samples were probed with specific primary antibodies: anti-PKCε (sc-1681, Santa Cruz Biotechnology, Inc. Dallas, TX, USA, 1:200), anti-phospho-S729-PKCε (#44-977G, Thermo Fisher Scientific, Waltham, MA, USA, 1:200); Alexa Fluor 488 Goat anti-rabbit and Alexa Fluor 594 Goat anti-mouse were used as secondary antibodies (Jackson Immuno-research). The analyses were performed by using confocal microscopy, as reported elsewhere [60]. The fluorescence was quantified by extrapolating the mean intensity of each channel from multiple regions of interest (ROI) and normalized to the background [12] by using the NIS-Elements AR (Advanced Research) software.

4.5. Cellular Viability Assay

Cell viability was assessed using the colorimetric reagent-based MTT cell proliferation kit I, based on the 3-[4,5-dimethylthiazol-2-yl]-2,5-diphenyltetrazolium bromide (Roche Diagnostics, Germany) salt, as previously described [58,61]. Briefly, after 24 hours from the doxycycline (2 µg/mL) induction, the cells were prompted to apoptosis by serum starvation or chemokines-induced toxicity (GROα, 1 ng/mL and MIP2α, 100 nM) (SRP4210 and SRP4251, Sigma-Aldrich, Munich, Germany). The cells were incubated for 10 min (pulse treatment) with Bryostatins-1 at different concentrations (100 pM, 1 nM, 10 nM and 100 nM, Calbiochem, Merck Millipore, Burlington, Massachusetts) and allowed to grow for 24 or 48 h. Subsequently, 0.5 mg/mL of MTT was added to each well and incubated for 4 h at 37 °C. The reaction was stopped by adding 100 µL of solubilization solution, then, formazan, formed by the cleavage of the yellow tetrazolium salt MTT, was measured spectrophotometrically by absorbance change at 550–600 nm using a microplate reader (BioRad (Hercules, CA, USA)). Six replicate wells were used for each group. The controls included untreated cells, whereas the medium alone was used as a blank.

4.6. Statistical Analysis

The data are represented as the mean ± standard error of the mean. *t*-tests and one-way analysis of variance were used to compare differences among groups, and statistical significance was assessed by the Tukey–Kramer post hoc test. The level of significance for all the statistical tests was set at $p \leq 0.05$. All the statistics were run using the Prism 5.0a (GraphPad Software Inc., La Jolla, CA, USA) software package.

5. Conclusions

Taken together, our findings suggest that PKCε alteration could play a role in ALS pathophysiology, and PKCε agonism by Bryostatins-1 may represent a potential neuroprotective strategy against motor neuronal degeneration in a specific subgroup of sporadic ALS patients. The evidence reported here suggests that cellular-based *in vitro* models may be suitable to investigate specific molecular subgroups, thus representing an interesting starting point for future preclinical and clinical studies aimed at developing patient-tailored pharmacological treatments.

Author Contributions: Conceptualization, D.L.A. and S.C.; data curation, V.L.C., A.G.D. and G.M. (Grazia Maugeri); formal analysis, V.L.C., A.G.D., G.M. (Grazia Maugeri) and V.D.; funding acquisition, S.C.; investigation, V.L.C., A.G.D., G.M. (Grazia Maugeri), G.M. (Giovanna Morello), M.G., B.M. and V.D.; methodology, V.L.C., A.G.D. and G.M. (Grazia Maugeri); resources, E.A.; supervision, V.D. and S.C.; writing—original draft, V.L.C.; writing—review and editing, V.L.C. and S.C. All authors have read and agreed to the published version of the manuscript.

Funding: This research was funded by the IRIB-CNR project “A multi-omics approach for the study of neurodegeneration” (grant number: DSB.AD007.304 to S.C). EA was supported by ALS Stichting (grant “ALS Tissue Bank–NL”).

Institutional Review Board Statement: The study was conducted in accordance with the Declaration of Helsinki, approved by an ethical committee (Ethics Committee of the Amsterdam Academic Medical Center, approved protocol: W11_073) for medical research and has been performed in accordance with ethical standards, as previously reported [16,62].

Informed Consent Statement: Informed consent was obtained from all individual participants included in the study for the use of tissue and for access to medical records for research purposes.

Data Availability Statement: Transcriptional data are available at EBI ArrayExpress database with the accession number E-MTAB-8635 (<https://www.ebi.ac.uk/arrayexpress/experiments/E-MTAB-8635/> accessed on 1 June 2021) and at the Gene Expression Omnibus with the accession number GSE124439 (<https://www.ncbi.nlm.nih.gov/geo/query/acc.cgi?acc=GSE124439> accessed on 1 January 2023).

Acknowledgments: The authors gratefully acknowledge Cristina Calì, Alfia Corsino, Maria Patrizia D’Angelo and Francesco Marino for their administrative and technical support.

Conflicts of Interest: The authors declare no conflict of interest.

References

1. Mathis, S.; Goizet, C.; Soulages, A.; Vallat, J.M.; Masson, G.L. Genetics of amyotrophic lateral sclerosis: A review. *J. Neurol. Sci.* **2019**, *399*, 217–226. [[CrossRef](#)] [[PubMed](#)]
2. Mitchell, J.D.; Borasio, G.D. Amyotrophic lateral sclerosis. *Lancet* **2007**, *369*, 2031–2041. [[CrossRef](#)] [[PubMed](#)]
3. Gentile, G.; Morello, G.; La Cognata, V.; Guarnaccia, M.; Conforti, F.L.; Cavallaro, S. Dysregulated miRNAs as Biomarkers and Therapeutic Targets in Neurodegenerative Diseases. *J. Pers. Med.* **2022**, *12*, 770. [[CrossRef](#)] [[PubMed](#)]
4. Gentile, G.; La Cognata, V.; Cavallaro, S. The contribution of CNVs to the most common aging-related neurodegenerative diseases. *Aging Clin. Exp. Res.* **2021**, *33*, 1187–1195. [[CrossRef](#)] [[PubMed](#)]
5. Rosen, D.R.; Siddique, T.; Patterson, D.; Figlewicz, D.A.; Sapp, P.; Hentati, A.; Donaldson, D.; Goto, J.; O’Regan, J.P.; Deng, H.X.; et al. Mutations in Cu/Zn superoxide dismutase gene are associated with familial amyotrophic lateral sclerosis. *Nature* **1993**, *362*, 59–62. [[CrossRef](#)] [[PubMed](#)]
6. Valentine, J.S.; Doucette, P.A.; Zittin Potter, S. Copper-zinc superoxide dismutase and amyotrophic lateral sclerosis. *Annu. Rev. Biochem.* **2005**, *74*, 563–593. [[CrossRef](#)]
7. Mulligan, V.K.; Chakrabartty, A. Protein misfolding in the late-onset neurodegenerative diseases: Common themes and the unique case of amyotrophic lateral sclerosis. *Proteins* **2013**, *81*, 1285–1303. [[CrossRef](#)]
8. Akçimen, F.; Lopez, E.R.; Landers, J.E.; Nath, A.; Chiò, A.; Chia, R.; Traynor, B.J. Amyotrophic lateral sclerosis: Translating genetic discoveries into therapies. *Nat. Rev. Genet.* **2023**, *24*, 642–658. [[CrossRef](#)]
9. Johnson, S.A.; Fang, T.; De Marchi, F.; Neel, D.; Van Weehaeghe, D.; Berry, J.D.; Paganoni, S. Pharmacotherapy for Amyotrophic Lateral Sclerosis: A Review of Approved and Upcoming Agents. *Drugs* **2022**, *82*, 1367–1388. [[CrossRef](#)]
10. Turner, M.R.; Parton, M.J.; Leigh, P.N. Clinical trials in ALS: An overview. *Semin. Neurol.* **2001**, *21*, 167–175. [[CrossRef](#)]
11. La Cognata, V.; Morello, G.; Cavallaro, S. Omics Data and Their Integrative Analysis to Support Stratified Medicine in Neurodegenerative Diseases. *Int. J. Mol. Sci.* **2021**, *22*, 4820. [[CrossRef](#)]
12. La Cognata, V.; Golini, E.; Iemmolo, R.; Balletta, S.; Morello, G.; De Rosa, C.; Villari, A.; Marinelli, S.; Vacca, V.; Bonaventura, G.; et al. CXCR2 increases in ALS cortical neurons and its inhibition prevents motor neuron degeneration in vitro and improves neuromuscular function in SOD1G93A mice. *Neurobiol. Dis.* **2021**, *160*, 105538. [[CrossRef](#)] [[PubMed](#)]
13. Morello, G.; Spampinato, A.G.; Cavallaro, S. Molecular Taxonomy of Sporadic Amyotrophic Lateral Sclerosis Using Disease-Associated Genes. *Front. Neurol.* **2017**, *8*, 152. [[CrossRef](#)] [[PubMed](#)]
14. Morello, G.; Spampinato, A.G.; Conforti, F.L.; D’Agata, V.; Cavallaro, S. Selection and Prioritization of Candidate Drug Targets for Amyotrophic Lateral Sclerosis Through a Meta-Analysis Approach. *J. Mol. Neurosci.* **2017**, *61*, 563–580. [[CrossRef](#)] [[PubMed](#)]
15. Tam, O.H.; Rozhkov, N.V.; Shaw, R.; Kim, D.; Hubbard, I.; Fennessey, S.; Propp, N.; Consortium, N.A.; Fagegaltier, D.; Harris, B.T.; et al. Postmortem Cortex Samples Identify Distinct Molecular Subtypes of ALS: Retrotransposon Activation, Oxidative Stress, and Activated Glia. *Cell Rep.* **2019**, *29*, 1164–1177 e1165. [[CrossRef](#)] [[PubMed](#)]

16. Aronica, E.; Baas, F.; Iyer, A.; ten Asbroek, A.L.; Morello, G.; Cavallaro, S. Molecular classification of amyotrophic lateral sclerosis by unsupervised clustering of gene expression in motor cortex. *Neurobiol. Dis.* **2015**, *74*, 359–376. [[CrossRef](#)] [[PubMed](#)]
17. Dave, K.R.; Raval, A.P.; Purroy, J.; Kirkinetzos, I.G.; Moraes, C.T.; Bradley, W.G.; Perez-Pinzon, M.A. Aberrant deltaPKC activation in the spinal cord of Wobbler mouse: A model of motor neuron disease. *Neurobiol. Dis.* **2005**, *18*, 126–133. [[CrossRef](#)]
18. Tury, A.; Tolentino, K.; Zou, Y. Altered expression of atypical PKC and Ryk in the spinal cord of a mouse model of amyotrophic lateral sclerosis. *Dev. Neurobiol.* **2014**, *74*, 839–850. [[CrossRef](#)]
19. Lanius, R.A.; Paddon, H.B.; Mezei, M.; Wagey, R.; Krieger, C.; Pelech, S.L.; Shaw, C.A. A role for amplified protein kinase C activity in the pathogenesis of amyotrophic lateral sclerosis. *J. Neurochem.* **1995**, *65*, 927–930. [[CrossRef](#)]
20. Guo, W.; Vandoorne, T.; Steyaert, J.; Staats, K.A.; Van Den Bosch, L. The multifaceted role of kinases in amyotrophic lateral sclerosis: Genetic, pathological and therapeutic implications. *Brain* **2020**, *143*, 1651–1673. [[CrossRef](#)]
21. Lanuza, M.A.; Just-Borrás, L.; Hurtado, E.; Cilleros-Mane, V.; Tomas, M.; Garcia, N.; Tomas, J. The Impact of Kinases in Amyotrophic Lateral Sclerosis at the Neuromuscular Synapse: Insights into BDNF/TrkB and PKC Signaling. *Cells* **2019**, *8*, 1578. [[CrossRef](#)] [[PubMed](#)]
22. Krieger, C.; Hu, J.H.; Pelech, S. Aberrant protein kinases and phosphoproteins in amyotrophic lateral sclerosis. *Trends Pharmacol. Sci.* **2003**, *24*, 535–541. [[CrossRef](#)] [[PubMed](#)]
23. Sipka, S.; Biro, T.; Czifra, G.; Griger, Z.; Gergely, P.; Brugos, B.; Tarr, T. The role of protein kinase C isoenzymes in the pathogenesis of human autoimmune diseases. *Clin. Immunol.* **2022**, *241*, 109071. [[CrossRef](#)] [[PubMed](#)]
24. Newton, P.M.; Messing, R.O. The substrates and binding partners of protein kinase Cepsilon. *Biochem. J.* **2010**, *427*, 189–196. [[CrossRef](#)]
25. Shirai, Y.; Adachi, N.; Saito, N. Protein kinase Cepsilon: Function in neurons. *FEBS J.* **2008**, *275*, 3988–3994. [[CrossRef](#)]
26. Van Kolen, K.; Pullan, S.; Neefs, J.M.; Dautzenberg, F.M. Nociceptive and behavioural sensitisation by protein kinase Cepsilon signalling in the CNS. *J. Neurochem.* **2008**, *104*, 1–13. [[CrossRef](#)]
27. Churchill, E.N.; Mochly-Rosen, D. The roles of PKCdelta and epsilon isoenzymes in the regulation of myocardial ischaemia/reperfusion injury. *Biochem. Soc. Trans.* **2007**, *35*, 1040–1042. [[CrossRef](#)]
28. Aksoy, E.; Goldman, M.; Willems, F. Protein kinase C epsilon: A new target to control inflammation and immune-mediated disorders. *Int. J. Biochem. Cell Biol.* **2004**, *36*, 183–188. [[CrossRef](#)]
29. Alkon, D.; Sun, M.K.; Thompson, R. Evidence of significant cognitive improvement over baseline in advanced Alzheimer's disease (AD) patients: A regenerative therapeutic strategy. *Alzheimers Dement.* **2021**, *17*, e050013. [[CrossRef](#)]
30. Etcheberrigaray, R.; Tan, M.; Dewachter, I.; Kuiperi, C.; Van der Auwera, I.; Wera, S.; Qiao, L.; Bank, B.; Nelson, T.J.; Kozikowski, A.P.; et al. Therapeutic effects of PKC activators in Alzheimer's disease transgenic mice. *Proc. Natl. Acad. Sci. USA* **2004**, *101*, 11141–11146. [[CrossRef](#)]
31. Xu, T.R.; He, G.; Dobson, K.; England, K.; Rumsby, M. Phosphorylation at Ser729 specifies a Golgi localisation for protein kinase C epsilon (PKCepsilon) in 3T3 fibroblasts. *Cell. Signal.* **2007**, *19*, 1986–1995. [[CrossRef](#)]
32. Nelson, T.J.; Sun, M.K.; Lim, C.; Sen, A.; Khan, T.; Chirila, F.V.; Alkon, D.L. Bryostatins Effects on Cognitive Function and PKCepsilon in Alzheimer's Disease Phase IIa and Expanded Access Trials. *J. Alzheimers Dis.* **2017**, *58*, 521–535. [[CrossRef](#)] [[PubMed](#)]
33. Ly, C.; Shimizu, A.J.; Vargas, M.V.; Duim, W.C.; Wender, P.A.; Olson, D.E. Bryostatin 1 Promotes Synaptogenesis and Reduces Dendritic Spine Density in Cortical Cultures through a PKC-Dependent Mechanism. *ACS Chem. Neurosci.* **2020**, *11*, 1545–1554. [[CrossRef](#)] [[PubMed](#)]
34. Reynolds, N.J.; Baldassare, J.J.; Henderson, P.A.; Shuler, J.L.; Ballas, L.M.; Burns, D.J.; Moomaw, C.R.; Fisher, G.J. Translocation and Downregulation of Protein Kinase C Isoenzymes- α and - ϵ by Phorbol Ester and Bryostatin-1 in Human Keratinocytes and Fibroblasts. *J. Investig. Dermatol.* **1994**, *103*, 364–369. [[CrossRef](#)]
35. Nagao, M.; Kato, S.; Oda, M.; Hirai, S. Decrease of protein kinase C in the spinal motor neurons of amyotrophic lateral sclerosis. *Acta Neuropathol.* **1998**, *96*, 52–56. [[CrossRef](#)] [[PubMed](#)]
36. Hu, J.H.; Chernoff, K.; Pelech, S.; Krieger, C. Protein kinase and protein phosphatase expression in the central nervous system of G93A mSOD over-expressing mice. *J. Neurochem.* **2003**, *85*, 422–431. [[CrossRef](#)] [[PubMed](#)]
37. Ferri, A.; Cozzolino, M.; Crosio, C.; Nencini, M.; Casciati, A.; Gralla, E.B.; Rotilio, G.; Valentine, J.S.; Carri, M.T. Familial ALS-superoxide dismutases associate with mitochondria and shift their redox potentials. *Proc. Natl. Acad. Sci. USA* **2006**, *103*, 13860–13865. [[CrossRef](#)]
38. Morello, G.; Spampinato, A.G.; Cavallaro, S. Neuroinflammation and ALS: Transcriptomic Insights into Molecular Disease Mechanisms and Therapeutic Targets. *Mediat. Inflamm.* **2017**, *2017*, 7070469. [[CrossRef](#)]
39. D'Amico, A.G.; Maugeri, G.; Saccone, S.; Federico, C.; Cavallaro, S.; Reglodi, D.; D'Agata, V. PACAP Modulates the Autophagy Process in an In Vitro Model of Amyotrophic Lateral Sclerosis. *Int. J. Mol. Sci.* **2020**, *21*, 2943. [[CrossRef](#)]
40. La Cognata, V.; D'Amico, A.G.; Maugeri, G.; Morello, G.; Guarnaccia, M.; Magri, B.; Aronica, E.; D'Agata, V.; Cavallaro, S. CXCR2 Is Deregulated in ALS Spinal Cord and Its Activation Triggers Apoptosis in Motor Neuron-Like Cells Overexpressing hSOD1-G93A. *Cells* **2023**, *12*, 1813. [[CrossRef](#)]
41. Tian, Z.; Lu, X.-T.; Jiang, X.; Tian, J. Bryostatin-1: A promising compound for neurological disorders. *Front. Pharmacol.* **2023**, *14*, 7411. [[CrossRef](#)]

42. Sunesson, L.; Hellman, U.; Larsson, C. Protein kinase Cepsilon binds peripherin and induces its aggregation, which is accompanied by apoptosis of neuroblastoma cells. *J. Biol. Chem.* **2008**, *283*, 16653–16664. [[CrossRef](#)] [[PubMed](#)]
43. Zeidman, R.; Pettersson, L.; Sailaja, P.R.; Truedsson, E.; Fagerstrom, S.; Pahlman, S.; Larsson, C. Novel and classical protein kinase C isoforms have different functions in proliferation, survival and differentiation of neuroblastoma cells. *Int. J. Cancer* **1999**, *81*, 494–501. [[CrossRef](#)]
44. Zeidman, R.; Lofgren, B.; Pahlman, S.; Larsson, C. PKCepsilon, via its regulatory domain and independently of its catalytic domain, induces neurite-like processes in neuroblastoma cells. *J. Cell. Biol.* **1999**, *145*, 713–726. [[CrossRef](#)]
45. Chen, Y.; Tian, Q. The role of protein kinase C epsilon in neural signal transduction and neurogenic diseases. *Front. Med.* **2011**, *5*, 70–76. [[CrossRef](#)]
46. Matsuzaki, S.; Szwedda, P.A.; Szwedda, L.I.; Humphries, K.M. Regulated production of free radicals by the mitochondrial electron transport chain: Cardiac ischemic preconditioning. *Adv. Drug Deliv. Rev.* **2009**, *61*, 1324–1331. [[CrossRef](#)]
47. Patten, S.A.; Sihra, R.K.; Dhami, K.S.; Coutts, C.A.; Ali, D.W. Differential expression of PKC isoforms in developing zebrafish. *Int. J. Dev. Neurosci.* **2007**, *25*, 155–164. [[CrossRef](#)]
48. Sen, A.; Nelson, T.J.; Alkon, D.L.; Hongpaisan, J. Loss in PKC Epsilon Causes Downregulation of MnSOD and BDNF Expression in Neurons of Alzheimer’s Disease Hippocampus. *J. Alzheimers Dis.* **2018**, *63*, 1173–1189. [[CrossRef](#)] [[PubMed](#)]
49. Wender, P.A.; Lipka, B.; Park, C.-M.; Irie, K.; Nakahara, A.; Ohigashi, H. Selective binding of bryostatin analogues to the cysteine rich domains of protein kinase C isozymes. *Bioorg. Med. Chem. Lett.* **1999**, *9*, 1687–1690. [[CrossRef](#)]
50. Lorenzo, P.S.; Bogi, K.; Hughes, K.M.; Beheshti, M.; Bhattacharyya, D.; Garfield, S.H.; Pettit, G.R.; Blumberg, P.M. Differential roles of the tandem C1 domains of protein kinase C delta in the biphasic down-regulation induced by bryostatin 1. *Cancer Res.* **1999**, *59*, 6137–6144. [[PubMed](#)]
51. Alkon, D.L.; Epstein, H.; Kuzirian, A.; Bennett, M.C.; Nelson, T.J. Protein synthesis required for long-term memory is induced by PKC activation on days before associative learning. *Proc. Natl. Acad. Sci. USA* **2005**, *102*, 16432–16437. [[CrossRef](#)] [[PubMed](#)]
52. Mizutani, K.; Sonoda, S.; Wakita, H.; Takahashi, Y. Effects of exercise and bryostatin-1 on functional recovery and posttranslational modification in the perilesional cortex after cerebral infarction. *NeuroReport* **2023**, *34*, 267–272. [[CrossRef](#)] [[PubMed](#)]
53. Chiu, I.M.; Morimoto, E.T.; Goodarzi, H.; Liao, J.T.; O’Keeffe, S.; Phatnani, H.P.; Muratet, M.; Carroll, M.C.; Levy, S.; Tavazoie, S.; et al. A neurodegeneration-specific gene-expression signature of acutely isolated microglia from an amyotrophic lateral sclerosis mouse model. *Cell Rep.* **2013**, *4*, 385–401. [[CrossRef](#)]
54. La Cognata, V.; Gentile, G.; Aronica, E.; Cavallaro, S. Splicing Players Are Differently Expressed in Sporadic Amyotrophic Lateral Sclerosis Molecular Clusters and Brain Regions. *Cells* **2020**, *9*, 159. [[CrossRef](#)] [[PubMed](#)]
55. Fetoni, A.R.; Zorzi, V.; Paciello, F.; Ziraldo, G.; Peres, C.; Raspa, M.; Scavizzi, F.; Salvatore, A.M.; Crispino, G.; Tognola, G.; et al. Cx26 partial loss causes accelerated presbycusis by redox imbalance and dysregulation of Nfr2 pathway. *Redox Biol.* **2018**, *19*, 301–317. [[CrossRef](#)]
56. Bonaventura, G.; Iemmolo, R.; D’Amico, A.G.; La Cognata, V.; Costanzo, E.; Zappia, M.; D’Agata, V.; Conforti, F.L.; Aronica, E.; Cavallaro, S. PACAP and PAC1R are differentially expressed in motor cortex of amyotrophic lateral sclerosis patients and support survival of iPSC-derived motor neurons. *J. Cell. Physiol.* **2018**, *233*, 3343–3351. [[CrossRef](#)]
57. Cashman, N.R.; Durham, H.D.; Blusztajn, J.K.; Oda, K.; Tabira, T.; Shaw, I.T.; Dahrouge, S.; Antel, J.P. Neuroblastoma x spinal cord (NSC) hybrid cell lines resemble developing motor neurons. *Dev. Dyn.* **1992**, *194*, 209–221. [[CrossRef](#)]
58. Maugeri, G.; D’Amico, A.G.; Rasa, D.M.; Federico, C.; Saccone, S.; Morello, G.; La Cognata, V.; Cavallaro, S.; D’Agata, V. Molecular mechanisms involved in the protective effect of pituitary adenylate cyclase-activating polypeptide in an in vitro model of amyotrophic lateral sclerosis. *J. Cell. Physiol.* **2019**, *234*, 5203–5214. [[CrossRef](#)]
59. Bonaventura, G.; Iemmolo, R.; Attaguile, G.A.; La Cognata, V.; Pistone, B.S.; Raudino, G.; D’Agata, V.; Cantarella, G.; Barcellona, M.L.; Cavallaro, S. iPSCs: A Preclinical Drug Research Tool for Neurological Disorders. *Int. J. Mol. Sci.* **2021**, *22*, 4596. [[CrossRef](#)]
60. Zohar, O.; Reiter, Y.; Bennink, J.R.; Lev, A.; Cavallaro, S.; Paratore, S.; Pick, C.G.; Brooker, G.; Yewdell, J.W. Cutting edge: MHC class I-Ly49 interaction regulates neuronal function. *J. Immunol.* **2008**, *180*, 6447–6451. [[CrossRef](#)]
61. D’Amico, A.G.; Scuderi, S.; Maugeri, G.; Cavallaro, S.; Drago, F.; D’Agata, V. NAP reduces murine microvascular endothelial cells proliferation induced by hyperglycemia. *J. Mol. Neurosci.* **2014**, *54*, 405–413. [[CrossRef](#)] [[PubMed](#)]
62. Morello, G.; Guarnaccia, M.; Spampinato, A.G.; Salomone, S.; D’Agata, V.; Conforti, F.L.; Aronica, E.; Cavallaro, S. Integrative multi-omic analysis identifies new drivers and pathways in molecularly distinct subtypes of ALS. *Sci. Rep.* **2019**, *9*, 9968. [[CrossRef](#)] [[PubMed](#)]

Disclaimer/Publisher’s Note: The statements, opinions and data contained in all publications are solely those of the individual author(s) and contributor(s) and not of MDPI and/or the editor(s). MDPI and/or the editor(s) disclaim responsibility for any injury to people or property resulting from any ideas, methods, instructions or products referred to in the content.